

# LOW-FREQUENCY MOTIONS IN PROTEIN MOLECULES

## $\beta$ -Sheet and $\beta$ -Barrel

KUO-CHEN CHOU

*Shanghai Institute of Biochemistry, Chinese Academy of Sciences, Shanghai, China*

**ABSTRACT** Low-frequency internal motions in protein molecules play a key role in biological functions. Based on previous work with  $\alpha$ -helical structure, the quasi-continuum model is extended to the  $\beta$ -structure, another fundamental element in protein molecules. In terms of the equations derived here, one can easily calculate the low-frequency wave number of a  $\beta$ -sheet in an accordionlike motion, and the low-frequency wave number of a  $\beta$ -barrel in a breathing motion. The calculated results for immunoglobulin G and concanavalin A agree well with the observations. These findings further verify that the observed low-frequency motion (or the so-called dominant low-frequency mode) in a protein molecule is essentially governed by the collective fluctuations of its weak bonds, especially hydrogen bonds, and the internal displacement of the massive atoms therein, as described by the quasi-continuum model.

### INTRODUCTION

According to both experimental (Brown et al., 1972; Fanconi and Finegold, 1975; Genzel et al., 1976; Painter et al., 1981, 1982; Evans et al., 1982; Pohl 1983) and theoretical progress in protein dynamics (Chou and Chen, 1977, 1978; Peticolas, 1979; Karplus and McCammon, 1981; Chou, 1983*a, b*; Gō et al., 1983; Chou, 1984*a, c*. Levy et al., 1984), it is clear that low-frequency internal motions do exist in protein and DNA molecules and indeed play a significant role in biological functions (Chou et al., 1981; Zhou, 1981; Chou, 1984*b*; Chou and Kiang, 1985); However, to fully understand the dynamic mechanism of those biological functions involved in the internal movements of protein, it is important to identify (Chou, 1983*b*) and furthermore predict (Chou, 1985) the dominant low-frequency mode (Chou, 1984*a*) for a given protein molecule with a known three-dimensional structure. The so-called dominant low-frequency mode corresponds to the maximum low-frequency peak observed for the protein molecule. If the final calculated result is just a frequency spectrum (Gō et al., 1983; Levy et al., 1984), then one still could not predict which was the dominant low-frequency mode. In other words, further physical treatments are needed in order to find the dominant low-frequency mode. It is also necessary to construct a physical model that describes the dominant low-frequency motion, which is actually the collective movement involving massive atoms in a protein molecule. In fact, we know that the dominant low-frequency mode possesses the largest amplitude and that the number of phonons (Chou and Chen, 1977; Chou, 1984*b*) excited at this frequency is overwhelming, and

therefore its contribution to free energy from phonon entropy is the greatest. That is why the dominant low-frequency motion is so important in biological functions, from the viewpoints of both thermodynamics (Chou and Chen, 1977, 1978) and molecular dynamics (Chou, 1984*b*). The study of low-frequency collective motion is also significant in revealing the essence of the activating low-frequency mode (Chou et al., 1981; Chou, 1983*a*; Chou, 1984*a*), an intriguing concept that associates the dominant low-frequency mode of a protein molecule with its internal conformation, and hence its biological activity.

Recently a set of physically intuitive and easily manipulated mathematical formulae were derived (Chou, 1983*a, b*; Chou, 1984*a, b*), by which the fundamental (lowest) frequency of an  $\alpha$ -helix in a protein molecule in different microenvironments can be calculated. The calculated results for  $\alpha$ -chymotrypsin, pepsin, insulin, and lysozyme are in very good agreement with the observations, as shown in Table I. This implies that the dominant low-frequency mode for each of these protein molecules actually originates from the accordionlike motion of the  $\alpha$ -helix (helices) described in column 2 of Table I. Despite the difference in the microenvironments of different protein molecules, these  $\alpha$ -helices have a common feature in length, i.e. usually consist of more than ten residues. This type of  $\alpha$ -helix is termed the principal helix (Chou, 1983*b*) so as to differentiate it from the other helices in a same protein molecule, which are either too short or in an unfavorable microenvironment (Chou, 1983*b*), and hence do not generate the dominant low-frequency motions. Moreover, this method was also used to predict (Chou, 1985) the dominant low-frequency mode for the bovine pancreatic trypsin inhibitor (BPTI) molecule although its observed result is not yet available.

In addition to agreeing well with the observations, the

Dr. Chou's present address is the Baker Laboratory of Chemistry, Cornell University, Ithaca, New York 14853.

TABLE I  
A COMPARISON BETWEEN THE OBSERVED LOW-FREQUENCY MODES FOR SOME PROTEINS AND THE CALCULATED RESULTS ACCORDING TO THE QUASI-CONTINUUM MODEL

Proteins	Principal structure involved	Form of motion	Calculated wave number	Observed wave number
$\alpha$ -Chymotrypsin	Helix (residues 235–245)	Accordionlike motion	$cm^{-1}$ 30*	$cm^{-1}$ 29‡
Pepsin	Helix (residues 225–235)	Accordionlike motion	33*	32‡
Insulin	Helix (residues B9–B19)	Accordionlike motion	23§	22
Lysozyme	{ Helix (residues 5–15) [ Helix (residues 25–35)	Accordionlike motion	27}§ 26}	25
Immunoglobulin-G	The $\beta$ -barrel consisting of nine strands in $V_H$ domain	Breathing motion	28**	28
Concanavalin A	The $\beta$ -barrel consisting of 14 strands	Breathing motion	19**	20

\*Chou, 1984a.

‡Brown et al., 1972.

§Chou, 1983b.

||Painter et al., 1982.

¶Genzel et al., 1976.

\*\*Examples illustrated in this paper.

calculation method has the following merits: (a) an intuitive and clear physical model, i.e., the accordionlike motion of a helix under different microenvironments in a protein molecule is explicitly depicted by the model itself as well as the process of deriving formulae. (b) The calculation is much easier and simpler in comparison with other methods (Karplus and McCammon, 1981; Gō et al., 1983; Levy et al., 1984). and can even be carried out without using a computer. The former is very important for the study of biological functions from dynamic point of view, while the latter makes the relevant quantitative calculation or estimation feasible even for a very complicated protein molecule. The reason such simplified calculations can yield such good results is that the physical model, although simple, reflects the essence of low-frequency motions in protein molecules, which is actually the existence of a series of weak bonds and a relatively large effective mass (Chou and Chen, 1977). Consequently, although some complex but inessential factors were neglected during the approximate treatment, the final results still were very close to the experimental observations. Apparently, this is because the inessential factors either cancelled each other or reached an internal mutual equilibrium in a shorter period of time in comparison with the period of the low-frequency motion, as implied in the continuity model (Chou, 1983a, b).

Nevertheless, besides the accordionlike motion of helical structures which is used to interpret some low-frequency internal motions in protein molecules, other types of low-frequency modes might also exist in protein molecules, depending on their individual internal structures. It is well known that the  $\alpha$ -helix and the  $\beta$ -sheet are two fundamental structures in protein molecules. Furthermore, the  $\beta$ -structure also contains a series of hydrogen bonds, and hence is likely to assume low-frequency motion. For example, an outstanding low-frequency peak was also observed

for immunoglobulin G and concanavalin A (Painter et al., 1982), respectively, neither of which, however, contained an  $\alpha$ -helix but only extensive  $\beta$ -structure regions. Therefore, as a further step, an investigation into the fundamental vibrations of the  $\beta$ -structures is necessary and the present study attempts to do just that.

### $\beta$ -SHEET

As mentioned above and supported by previous calculations (Chou, 1983a, b; Chou, 1984a, b, c), one reason for low-frequency motions, which occur in protein and DNA molecules, is the existence of a series of weak bonds, such as hydrogen bonds. Consequently, while establishing a model to deal with this kind of internal movement, we must focus our attention on the essential aspects of the matter and neglect the inessential aspects. Whether we can correctly realize this is the key to the problem.

First we consider a vibration system consisting of rods and springs as illustrated in Fig. 1. Suppose  $m$  is the mass of each rod, and  $k$  the force constant of each spring whose mass is negligible. When such a system is in accordionlike motion, the fundamental (lowest) frequency can be derived as follows. Suppose  $2\zeta$  is the maximum stretch between two adjacent rods. Thus, the vibrational displacements of rods 1, 2, 3, 4, 5, 6 (Fig. 1) can be described by

$$\left. \begin{aligned} u_1(t) &= -5\zeta \sin \omega t \\ u_2(t) &= -3\zeta \sin \omega t \\ u_3(t) &= -\zeta \sin \omega t \\ u_4(t) &= \zeta \sin \omega t \\ u_5(t) &= 3\zeta \sin \omega t \\ u_6(t) &= 5\zeta \sin \omega t \end{aligned} \right\}, \quad (1)$$

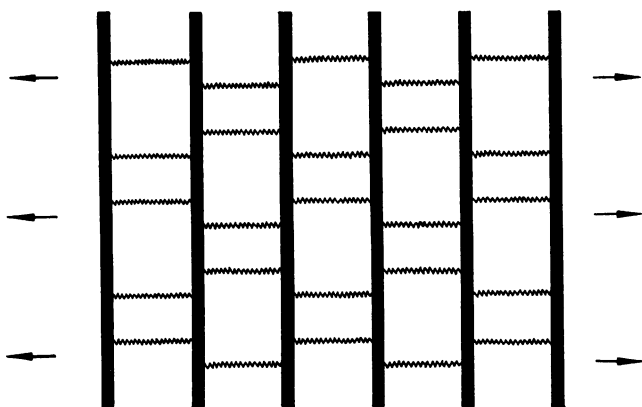


FIGURE 1 Vibration system with six rods and five springs between any two adjacent rods. The so-called rods and springs sheet.

respectively, where  $\omega$  is the circular frequency of the accordionlike vibration. The total maximum kinetic energy of the vibration system is then

$$\begin{aligned} \max T &= \sum_{i=1}^6 \frac{m}{2} \max \left[ \frac{du_i(t)}{dt} \right]^2 \\ &= \frac{m}{2} \omega^2 \zeta^2 (5^2 + 3^2 + 1^2 + 1^2 + 3^2 + 5^2) \\ &= 35m\omega^2 \zeta^2. \end{aligned} \quad (2)$$

On the other hand, the total maximum potential energy is (Chou, 1984a):

$$\begin{aligned} \max U &= \frac{5k}{2} [(2\zeta)^2 + (2\zeta)^2 \\ &\quad + (2\zeta)^2 + (2\zeta)^2 + (2\zeta)^2] = 50k\zeta^2. \end{aligned} \quad (3)$$

According to energy conservation, namely,  $\max T = \max U$ , we obtain the following expression for calculating the low-frequency mode of the system in Fig. 1:

$$\tilde{\nu} = \frac{\nu}{c} = \frac{\omega}{2\pi c} = \frac{1}{2\pi c} \sqrt{\frac{10k}{7m}}, \quad (4)$$

where  $\nu$  and  $\tilde{\nu}$  are the corresponding frequency and wave number, respectively, and  $c$  the speed of light in vacuum.

A general derivation by means of induction for this kind of systems will give

$$\tilde{\nu} = \begin{cases} \frac{1}{2\pi c} \sqrt{\frac{2(\mu-1)\lambda k}{[1^2 + 3^2 + \dots + (\mu-1)^2]m}} & \text{if } \mu \text{ is an even number} \\ \frac{1}{2\pi c} \sqrt{\frac{2(\mu-1)\lambda k}{[2^2 + 4^2 + \dots + (\mu-1)^2]m}} & \text{if } \mu \text{ is an odd number,} \end{cases} \quad (5)$$

where  $\mu$  is the number of rods, and  $\lambda$  the number of springs

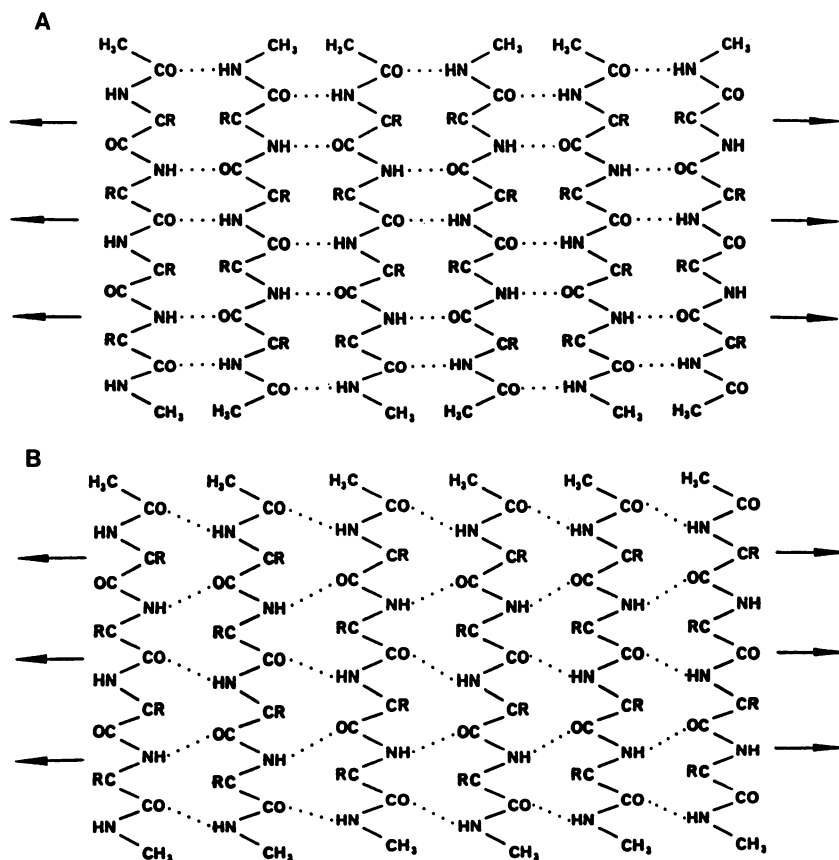


FIGURE 2 Schematic drawing for (A) an antiparallel  $\beta$ -sheet as symbolized by  $\beta_A[\text{COCH}_3-(\text{R})_4-\text{NHCH}_3]_6$ , and (B) a parallel  $\beta$ -sheet symbolized by  $\beta_P[\text{COCH}_3-(\text{R})_4-\text{NHCH}_3]_6$ . Note that in both cases the hydrogens bound to the  $\alpha$ -carbon atoms are omitted.

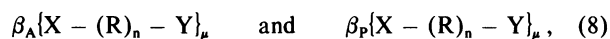
between two adjacent rods, which, e.g., are 6 and 5, respectively, for the case illustrated in Fig. 1. According to the following formulae

$$\left. \begin{aligned} 1^2 + 3^2 + \dots + (2J - 1)^2 &= J(4J^2 - 1)/3 \\ 2^2 + 4^2 + \dots + (2J)^2 &= 2J(J + 1)(2J + 1)/3 \end{aligned} \right\} \quad (6)$$

Eq. 5 can be further reduced to

$$\tilde{\nu} = \frac{1}{\pi c} \sqrt{\frac{3\lambda k}{\mu(\mu + 1)m}} \quad (7)$$

Now let us consider the  $\beta$ -sheet structures. For brevity, an antiparallel and parallel  $\beta$ -sheet is represented by



respectively, where X and Y denote the end groups, R represents any amino-acid residue,  $n$  is the number of residues in each chain, and  $\mu$  is the number of the constituent chains. The illustrations for  $\beta_A \{COCH_3 - (R)_4 - NHCH_3\}_6$  and  $\beta_P \{COCH_3 - (R)_4 - NHCH_3\}_6$  are given in Fig. 2 A and B, respectively. By comparing Figs. 1 and 2, we obtain the following three points. (a) The chains in Fig. 2 can be compared with the rods in Fig. 1. (b) The springs in Fig. 1 correspond to the hydrogen bonds in Fig. 2 A. Hence when Eq. 7 is applied to deal with an antiparallel  $\beta$ -sheet, we should substitute the force constant  $k$  with the stretching force constant of a hydrogen bond  $k_H^S$  (Itoh and Shimanouchi, 1970); i.e.,

$$k = k_H^S = 0.13 \times 10^5 \text{ dyn/cm}. \quad (9)$$

But the hydrogen bonds in Fig. 2 B tilt with an angle of  $\sim 20^\circ$  (Hol et al., 1981) with the direction of the accordion-like vibration, and hence for the parallel  $\beta$ -sheet we should instead have

$$k = \sqrt{(k_H^S \cos 20^\circ)^2 + (k_H^B \sin 20^\circ)^2} = 0.12 \times 10^5 \text{ dyn/cm}, \quad (10)$$

where  $k_H^B = 0.03 \times 10^5 \text{ dyn/cm}$  (Itoh and Shimanouchi, 1970) is the bending force constant of a hydrogen bond. (c) The number of hydrogen bonds in Fig. 2 is equal to  $n + 1$ , and therefore

$$\lambda = n + 1. \quad (11)$$

Now we use the equations derived here to calculate a typical representative of the  $\beta$ -sheets in proteins. The frequencies of 20 amino acids in the known  $\beta$ -structures are given in Table II (Lifson and Sander, 1979) from which the average mass per amino-acid residue can be obtained as follows:

$$\langle m_R \rangle = \frac{\sum_{i=1}^{20} f_i m_{R_i}}{\sum_{i=1}^{20} f_i} = 111 \text{ g/N}, \quad (12)$$

TABLE II  
THE FREQUENCIES OF 20 AMINO ACIDS IN THE KNOWN  $\beta$ -SHEETS

	Amino acid residue $R_i$	Frequency (%) $f_i$	Mass (amu) $m_{R_i}$
$i = 1$	Val	14.1	99
2	Leu	9.2	113
3	Ile	8.3	113
4	Ala	7.8	71
5	Thr	7.6	101
6	Ser	7.4	87
7	Gly	5.7	57
8	Tyr	5.7	163
9	Lys	5.0	129
10	Phe	4.4	147
11	Gln	3.2	128
12	Glu	2.9	129
13	Cys	2.7	103
14	Arg	2.6	157
15	Trp	2.6	186
16	Asp	2.5	115
17	Asn	2.5	114
18	His	2.3	138
19	Pro	1.8	98
20	Met	1.7	131

where  $m_{R_i}$  is the mass of the amino-acid residue  $R_i$ , and  $N$  the Avogadro constant. The statistical analysis for the known  $\beta$ -sheets indicates (Sternberg and Thornton, 1977) that the average number of chains per sheet is 4.7, and the observed distribution has a peak at 5–7 residues per chain. Therefore, as a representative for the  $\beta$ -sheets, we use the following parameters to calculate its fundamental frequency

$$\left. \begin{aligned} m &= 6 \langle m_R \rangle = 666 \text{ g/N} \\ \mu &= 5, \quad \lambda = n + 1 = 7 \end{aligned} \right\} \quad (13)$$

Substituting Eq. 13, as well as Eqs. 9 and 10, respectively, into Eq. 7, we obtain

$$\tilde{\nu} = \frac{1}{\pi \times 3 \times 10^{10}} \sqrt{\frac{3 \times 7 \times k \times 6.02 \times 10^{23}}{5 \times (5 + 1) \times 666}} = \begin{cases} 30.4 \text{ cm}^{-1} & \text{(for the antiparallel case)} \\ 29.2 \text{ cm}^{-1} & \text{(for the parallel case),} \end{cases} \quad (14)$$

which means that a  $\beta$ -sheet with a certain size, such as the one given above, can also generate a low-frequency mode of  $\sim 30 \text{ cm}^{-1}$ . This is an instructive and enlightening finding. The slight difference between the two results in Eq. 14 also tells us that the effect due to a tilted angle of  $\sim 20^\circ$  in hydrogen bonds is trivial in affecting the calculated low-frequency mode. Consequently, it will be unnecessary later to differentiate between the hydrogen bond in an antiparallel sheet and that in a parallel sheet when using Eq. 7. This also justifies the approximate validity of the present model even for a twist  $\beta$ -sheet (Chou and Schera-

ga, 1982). Furthermore, Eq. 7 can be approximately extended to deal with a nonregular  $\beta$ -sheet if the nonregularity does not cause great relative variance in  $\langle m \rangle$ , the average mass of a strand, and in  $\langle \lambda \rangle_s$ , the average number of hydrogen bonds between two adjacent strands in a nonregular  $\beta$ -sheet. In this case, we extend Eq. 7 to

$$\bar{v} \approx \frac{1}{\pi c} \sqrt{\frac{3\Lambda_s k}{(\mu^2 - 1)M}}, \quad (15)$$

where  $\Lambda_s = (\mu - 1)\langle \lambda \rangle_s$  is the number of the total hydrogen bonds of a nonregular  $\beta$ -sheet, and  $M = \mu \langle m \rangle$  is the total mass. Actually for many  $\beta$ -sheets in proteins, the above condition holds.

### $\beta$ -BARREL

Imagine that the rods and springs sheet in Fig. 1 is rolled up to form a barrel, which is then fixed by five additional springs between the first and last rods, as illustrated in Fig. 3. When such a barrel moves in a breathing motion its fundamental frequency can be derived as follows.

Fig. 4 is a schematic drawing describing the breathing motion of the barrel of Fig. 3 when viewed from its top. Assuming  $\xi$  is the maximum deviation of each rod from its own equilibrium position during the breathing motion, then

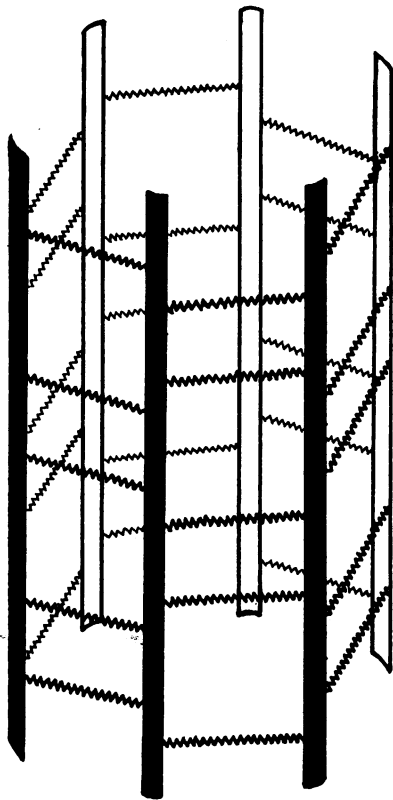


FIGURE 3 The rods and springs barrel formed by rolling up the rods and springs sheet of Fig. 1 and fixed by five additional springs between the first and last rods.

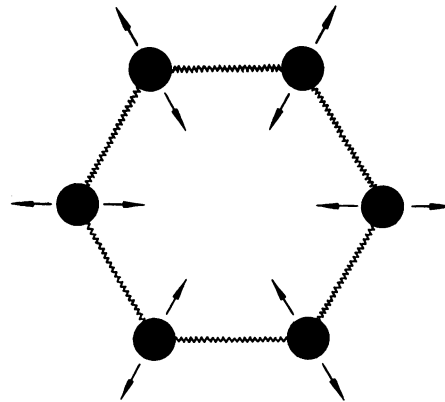


FIGURE 4 Schematic drawing for the breathing motion of the barrel in Fig. 3 when viewed from its top to bottom.

the displacement of the  $i$ th ( $i = 1, 2, \dots, 6$ ) rod along the direction as shown in Fig. 4 at any time can be described by

$$u_i(t) = \xi \sin \omega t \quad (i = 1, 2, \dots, 6), \quad (16)$$

which, however, will bring about a change in the distance between two adjacent rods, as given by

$$\begin{aligned} \Delta_{i(i+1)}(t) &= |u_i(t)u_{i+1}(t)| - |u_i(0)u_{i+1}(0)| \\ &= 2\xi \sin(\pi/6) \sin \omega t \\ (i &= 1, 2, \dots, 6; \quad i + 1 = 1 \quad \text{when } i = 6), \end{aligned} \quad (17)$$

where  $|u_i u_{i+1}|$  represents the distance between the  $i$ th and  $(i + 1)$ th rods. Thus, the total maximum kinetic energy of the system in such a breathing motion is

$$\max T = \frac{m}{2} \sum_{i=1}^6 \max \left[ \frac{du_i(t)}{dt} \right]^2 = 3m\omega^2 \xi^2 \quad (18)$$

and the total maximum potential energy, however, is

$$\max U = \frac{5k}{2} \sum_{i=1}^6 \max [\Delta_{i(i+1)}(t)]^2 = 60k \left( \sin \frac{\pi}{6} \right)^2 \xi^2. \quad (19)$$

According to energy conservation, i.e.,  $\max T = \max U$ , it follows

$$\bar{v} = \frac{\omega}{2\pi c} = \frac{1}{\pi c} \left( \sin \frac{\pi}{6} \right) \sqrt{\frac{5k}{m}}. \quad (20)$$

The above derivation can be easily extended to a general case; i.e., for a rods and springs barrel in which there are  $\mu$  rods and  $\lambda$  springs between any two adjacent rods, we generally have

$$\bar{v} = \frac{1}{\pi c} \left( \sin \frac{\pi}{\mu} \right) \sqrt{\frac{\lambda k}{m}}. \quad (21)$$

On the other hand, a  $\beta$ -barrel can also be formed by rolling up the  $\beta$ -sheet in Fig. 2. Accordingly, Eq. 21 can

also be used to calculate the breathing frequency of a regular  $\beta$ -barrel in which there are  $\mu$  strands and  $\lambda$  hydrogen bonds between any two adjacent strands. However, the  $m$  in Eq. 21 should be substituted by the mass of a strand, and  $k$  by the stretching force constant of a hydrogen bond.

However, when a  $\beta$ -barrel is nonregular, a similar extension as given above for a nonregular  $\beta$ -sheet will give

$$\tilde{\nu} \approx \frac{1}{\pi c} \left( \sin \frac{\pi}{\mu} \right) \sqrt{\frac{\Delta_b k}{M}}, \quad (22)$$

where  $\Delta_b$  is the number of the total hydrogen bonds in a  $\beta$ -barrel, and  $M$  its total mass. Also Eq. 22 is valid if there is no great relative variance in those two quantities as mentioned above; i.e., although the constituent amino-acid residues for each strand of a nonregular  $\beta$ -barrel might be much different, the mutual fluctuations thus caused in the mass of each strand and in the number of hydrogen bonds between any two adjacent strands are not too large. In fact, such a condition can also be satisfied for many  $\beta$ -barrels in proteins. Now let us employ Eq. 22 to treat some concrete protein molecules.

### Immunoglobulin G

It is well known that the antibody molecule IgG contains no  $\alpha$ -helix but does contain extensive  $\beta$ -structures. One striking feature of this molecule is that it is made up of 12 distinct domains (Beale and Feinstein, 1976; Padlan, 1977), each of which contains a  $\beta$ -barrel (Saul et al., 1978). For example, a stereo drawing of the  $\alpha$ -carbon backbone of its  $V_H$  domain (Saul et al., 1978) is given in Fig. 5, from which we can see the  $\beta$ -barrel therein consists of 9 strands. Therefore, we can substitute  $\mu = 9$ ,  $M \approx 6,440$  g/N, the mass of the  $\beta$ -barrel (Saul et al., 1978),  $\Delta_b = 50$ , the number of the total hydrogen bonds in the  $\beta$ -barrel (Saul et al., 1978), and  $k = 0.13 \times 10^5$  dyn/cm, the stretching force constant of a hydrogen bond (Itoch and Shimanouchi, 1970) into Eq. 22, and immediately

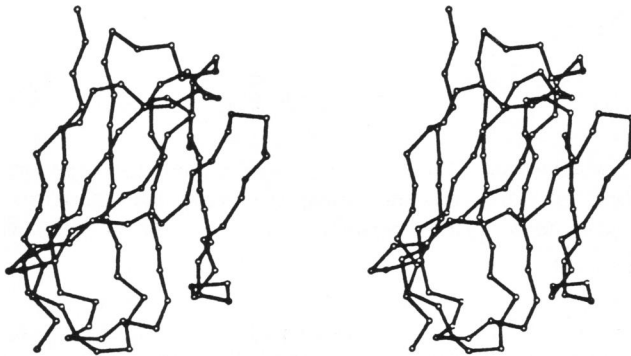


FIGURE 5 Stereo drawing of the  $\alpha$ -carbon backbone of the  $V_H$  domain in immunoglobulin G.

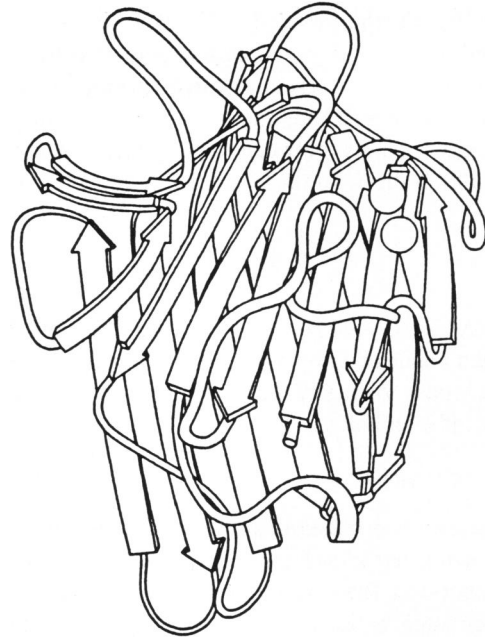


FIGURE 6 Schematic drawing of concanavalin A.

obtain

$$\tilde{\nu} \approx \frac{1}{\pi \times 3 \times 10^{10}} \left( \sin \frac{\pi}{9} \right) \cdot \sqrt{\frac{50 \times 0.13 \times 10^5 \times 6.02 \times 10^{23}}{6,440}} = 28.3 \text{ cm}^{-1}, \quad (23)$$

which is in an excellent agreement with the experimental observation of  $28 \text{ cm}^{-1}$  (Painter et al., 1982) for this protein molecule.

### Concanavalin A

The molecule has been widely used as a molecular probe in studies of cell membrane dynamics and cell division. Because of its arrangement of  $\beta$ -structures and distribution of hydrogen bonds, concanavalin A is classified as Greek key  $\beta$ -barrel (Richardson, 1981), whose schematic drawing is given in Fig. 6. For such a  $\beta$ -barrel, we have  $\mu = 14$ ,  $M \approx 13,320$  g/N as obtained from the Brookhaven Protein Data Bank (Bernstein et al., 1977) in April 1981, and  $\Delta_b = 110$  (Reeke et al., 1975). Then using Eq. 22, we have

$$\tilde{\nu} \approx \frac{1}{\pi \times 3 \times 10^{10}} \left( \sin \frac{\pi}{14} \right) \cdot \sqrt{\frac{110 \times 0.13 \times 10^5 \times 6.02 \times 10^{23}}{13,320}} = 19.0 \text{ cm}^{-1}, \quad (24)$$

which is close to the corresponding experimental observation of  $20 \text{ cm}^{-1}$  (Painter et al., 1982). For a simple and complete summary, all the above results are included in Table I.

## LOW-FREQUENCY AMPLITUDE

It is well known that an oscillator with frequency  $\nu$  will excite phonons each having energy of  $h\nu$ . Since phonons are bosons (Chou and Chen, 1977), under thermal equilibrium the mean number of phonons thus excited is, according to Bose-Einstein statistics, given by

$$\langle n_{\text{phonon}} \rangle = \frac{1}{\exp(h\nu/k_{\text{B}}T) - 1}, \quad (25)$$

where  $k_{\text{B}}$  is the Boltzmann constant,  $h$  the Planck constant, and  $T$  the absolute temperature. Thus, the average vibration energy of the oscillator is

$$\langle E \rangle = \langle n_{\text{phonon}} \rangle h\nu = \frac{h\nu}{\exp(h\nu/k_{\text{B}}T) - 1}, \quad (26)$$

which should equal to  $\max U$  according to energy conservation. Consequently, we obtain

$$\begin{aligned} A_{\beta-s} &= (\mu - 1)(2\xi) = 2(\mu - 1) \sqrt{\frac{\langle E \rangle}{2(\mu - 1)\lambda k}} \\ &= \sqrt{\frac{2(\mu - 1)h\nu}{\lambda k [\exp(h\nu/k_{\text{B}}T) - 1]}} \Big|_{h\nu \ll k_{\text{B}}T} \\ &\approx \sqrt{\frac{2(\mu - 1)k_{\text{B}}T}{\lambda k}} = (\mu - 1) \sqrt{\frac{2k_{\text{B}}T}{\Lambda_s k}} \end{aligned} \quad (27)$$

$$\begin{aligned} A_{\beta-b} &= 2\xi = 2 \sqrt{\frac{\langle E \rangle}{2\mu\lambda k \sin^2 \frac{\pi}{\mu}}} \\ &= \frac{1}{\sin(\pi/\mu)} \sqrt{\frac{2h\nu}{\mu\lambda k [\exp(h\nu/k_{\text{B}}T) - 1]}} \Big|_{h\nu \ll k_{\text{B}}T} \\ &\approx \frac{1}{\sin(\pi/\mu)} \sqrt{\frac{2k_{\text{B}}T}{\mu\lambda k}} = \frac{1}{\sin(\pi/\mu)} \sqrt{\frac{2k_{\text{B}}T}{\Lambda_b k}}, \end{aligned} \quad (28)$$

where  $A_{\beta-s}$  is the amplitude of a  $\beta$ -sheet in accordionlike motion, and  $A_{\beta-b}$  the amplitude of a  $\beta$ -barrel in breathing motion. Note that for low-frequency phonons whose wave numbers are  $< 50 \text{ cm}^{-1}$ , we generally have  $h\nu \ll k_{\text{B}}T$  at room temperature. For example, for the representative anti-parallel and parallel  $\beta$ -sheets as discussed above, when  $T = 300^\circ\text{K}$ , Eq. 27 will yield  $A_{\beta-s} = 0.19$  and  $0.20 \text{ \AA}$ , respectively, which are the amplitudes of the corresponding  $\beta$ -sheets in the accordion like motions. In using Eq. 28, we derive the amplitudes of the breathing motions occurring at the same temperature in the  $\beta$ -barrels in IgG and concanavalin A, respectively; they are  $A_{\beta-b} = 0.10$  and  $0.11 \text{ \AA}$ .

## DISCUSSION

### Comparison of the Existing Models

Since low-frequency internal motions were observed for some protein molecules (Brown et al., 1972), various

models have been proposed that attempt to reveal the possible mechanisms. They are roughly classified as follows.

(a) *The Elastic Global Model (Suzaki and Gō, 1975)*. In this model a protein molecule was compared with a continuous elastic sphere imitating heartbeat breathing motion, and the following formula from earth dynamics was used to calculate the low-frequency wave number for a globular protein

$$\tilde{\nu} = \frac{\nu}{c} = \frac{1}{2\pi c} \sqrt{\frac{\pi E}{\rho r^2}}, \quad (29)$$

where  $E$ ,  $\rho$ , and  $r$  are the Young's modulus, mass density, and radius of the protein molecule, respectively. This is a model full of imagination and has stimulated other developments in this field, both theoretical and experimental. However, since this model does not deal with internal conformation, the sensitive variation (Brown et al., 1972) of the observed low-frequency peak for a protein with conformational change cannot be seen, nor can the difference in the observed low-frequency wave numbers for different proteins be interpreted by Eq. 29. A detailed discussion of this model was given by Painter et al. (1982) and Chou (1983b), respectively.

(b) *The Normal Mode Model (Karplus and McCammon, 1981; Gō et al., 1983; Levy et al., 1984)*. This model is actually a combination of the classic normal mode theory with the modern computer technique. In principle it reaches the level of the constituent atoms in a protein molecule, and hence much more detailed information can be provided. But the application is much more complicated. The results thus obtained are very sensitive to the choice or assumption of the atomically potential functions, which, however, were based on semi-empirical principles. Consequently, in the long term, much work can be done following such a procedure, especially in improving the potential functions as well as the computation technique. Probably because of the technique's formidable complexity, no reports as yet have dealt with the  $\beta$ -barrel. Besides, this approach does not directly give the dominant low-frequency mode (i.e., the mode corresponding to the outstanding low-frequency peak observed) but a frequency spectrum. Therefore, further treatments are needed to find out the dominant low-frequency motion crucial in the study of biological functions.

(c) *The Quasi-Continuum Model (Chou, 1983a, b; 1984a)*. This model is situated between the elastic model and the normal mode model and hence can serve as a vehicle for the middle-range goal. Unlike the elastic global model, this model can, to some extent, reflect the

internal conformation and the microenvironment of a protein molecule. On the other hand, based on the physical character of low-frequency motion (Chou, 1984a), the constituent atoms are treated as continuous mass distributed according to geometric shape (conformation), thus greatly simplifying the problem in comparison with the discrete normal mode model. Consequently, a set of physically intuitive formulae have been derived to estimate the possible dominant low-frequency motions in a protein molecule and analyze their biological functions (Chou, 1984a, b).

(d) *The Amorphous Model* (Painter et al., 1982). This model illustrates that the broad low-frequency Raman scattering reflects the density of vibrational states of amorphous polymers. This is an attractive model, very useful in understanding the broadening of the observed low-frequency peak, and thus appropriately describing the relevant background. However, as pointed out by Painter et al. (1982), "such as interpretation does not rule out, and may be complementary with, other explanations."

In general, the four models presented above have stimulated, although at different levels, developments in this field. Because each model has its own criteria, perhaps a combination of characteristics from each model, successfully brought together to complement each other, could further our understanding of this kind of internal motion and its biological functions.

## CONCLUSION

We demonstrated that the accordionlike motion of a  $\beta$ -sheet and the breathing motion of a  $\beta$ -barrel can also generate the low-frequency modes of 20–30  $\text{cm}^{-1}$ . Good agreement between the observed and the calculated results indicates that a series of weak bonds, such as hydrogen bonds, and a substantial molecular mass distributed over the region of those weak bonds (Chou and Chen, 1977) are the two most essential factors for the low-frequency internal motions observed recently in more and more protein molecules. The physical model used here, although quite simple, does illustrate this kind of low-frequency internal motion. These findings are important in understanding the biological functions.

An enlightening discussion with Professor Tatsuo Ooi of Kyoto University is gratefully acknowledged.

Part of this paper was presented by the author at a seminar held at the Kyoto University, Japan, and the seminar at the Los Alamos National Laboratory, USA.

Received for publication 30 May 1984 and in final form 2 April 1985.

## REFERENCES

- Beale, D., and A. Feinstein. 1976. Structure and function of the regions of immunoglobulins. *Q. Rev. Biophys.* 9:135–180.
- Bernstein, F. C., T. F. Koetzle, G. J. B. Williams, E. F. Meyer, Jr., M. D. Brice, J. R. Rodgers, O. Kennard, T. Shimanouchi, and M. Tasumi. 1977. The protein data bank: a computer-based archival file for macromolecular structures. *J. Mol. Biol.* 112:535–542.
- Brown, K. G., S. C. Erfurth, E. W. Small, and W. L. Peticolas. 1972. Conformationally dependent low-frequency motions of proteins by laser Raman spectroscopy. *Proc. Natl. Acad. Sci. USA.* 69:1467–1469.
- Chou, K. C. 1983a. Low-frequency vibrations of helical structures in protein molecules. *Biochem. J.* 209:573–580.
- Chou, K. C. 1983b. Identification of low-frequency modes in protein molecules. *Biochem. J.* 215:465–469.
- Chou, K. C. 1984a. The biological functions of low-frequency vibrations (phonons). III. Helical structures and microenvironment. *Biophys. J.* 45:881–890.
- Chou, K. C. 1984b. The biological functions of low-frequency vibrations (phonons). IV. Resonance effects and allosteric transition. *Biophys. Chem.* 20:61–71.
- Chou, K. C. 1984c. Low-frequency vibrations of DNA molecules. *Biochem. J.* 221:27–31.
- Chou, K. C. 1985. Prediction of a low-frequency mode in BPTI molecule. *Int. J. Biol. Macromol.* In press.
- Chou, K. C., and N. Y. Chen. 1977. The biological functions of low-frequency phonons. *Sci. Sin.* 20:447–457.
- Chou, K. C., and N. Y. Chen. 1978. Some problems in quantum biology. *Huaxue Tongbao.* 5:29–34.
- Chou, K. C., and H. A. Scheraga. 1982. Origin of the right-handed twist of  $\beta$ -sheets of poly(L-Val) chains. *Proc. Natl. Acad. Sci. USA.* 79:7047–7051.
- Chou, K. C., and Y. S. Kiang. 1985. The biological functions of low-frequency vibrations (phonons). V. A phenomenological theory. *Biophys. Chem.* In press.
- Chou, K. C., N. Y. Chen, and S. Forsén. 1981. The biological functions of low-frequency phonons. II. Cooperative effects. *Chem. Scr.* 18:126–132.
- Evans, G. L., M. W. Evans, and R. Pething. 1982. The far infrared spectra of proteins and enzymes in the solid state. *Spectrochim. Acta. Part A. Mol. Spectrosc.* 38:421–422.
- Fanconi, B., and L. Finegold. 1975. Vibrational states of the biopolymer polyglycine. *Science (Wash. DC).* 190:458–460.
- Genzel, L., F. Keilman, T. P. Martin, G. Winterling, Y. Yacoby, H. Fröhlich and M. W. Makinen. 1976. Low-frequency Raman spectra of lysozyme. *Biopolymers.* 15:219–225.
- Gō, N., T. Noguti, and T. Nishikawa. 1983. Dynamics of a small globular protein in terms of low-frequency vibrational modes. *Proc. Natl. Acad. Sci. USA.* 80:3696–3700.
- Hol, W. G. J., L. M. Halie, and C. Sander. 1981. Dipoles of the  $\alpha$ -helix and  $\beta$ -sheet: Their role in protein folding. *Nature (Lond.).* 294:532–536.
- Itoh, K., and T. Shimanouchi. 1970. Vibrational frequencies and modes of  $\alpha$ -helices. *Biopolymers.* 9:383–399.
- Karplus, M., and J. A. McCammon. 1981. The internal dynamics of globular proteins. *CRC Crit. Rev. Biochem.* 9:293–349.
- Levy, R. M., A. R. Srinivasam, W. K. Olson, and J. A. McCammon. 1984. Quasi-harmonic method for studying very low frequency modes in proteins. *Biopolymers.* 23:1099–1112.
- Lifson, S., and C. Sander. 1979. Antiparallel and parallel  $\beta$ -strands differ in amino acid residue preferences. *Nature (Lond.).* 282:109–111.
- Padlan, E. A. 1977. Structural basis for the specificity of antibody-antigen reactions and structural mechanisms for the diversification of antigen-binding specificities. *Q. Rev. Biophys.* 10:35–65.
- Painter, P. C., L. E. Mosher, and C. Rhoads. 1981. "Low-frequency modes in the Raman spectrum of DNA. *Biopolymers.* 20:243–247.
- Painter, P. C., L. E. Mosher, and C. Rhoads. 1982. Low-frequency modes in the Raman spectra of proteins. *Biopolymers.* 21:1469–1472.
- Peticolas, W.L. 1979. Mean-square amplitudes of the longitudinal vibrations of helical polymers. *Biopolymers.* 18:747–755.
- Pohl, H. A. 1983. Natural oscillating fields of cells. *In Coherent Excita-*



- tion in Biological Systems. H. Fröhlich and F. Kremer, editors. Springer-Verlag, Berlin and Heidelberg. 199–210.
- Reeke, G. N., Jr., J. W. Becker, and G. M. Edelman. 1975. The covalent and three-dimensional structure of concanavalin A. *J. Biol. Chem.* 250:1525–1547.
- Richardson, J. S. 1981. The anatomy and taxonomy of protein structure. *Adv. Protein Chem.* 34:167–339.
- Saul, F. A., L. M. Amzel, and R. J. Poljak. 1978. Preliminary refinement and structural analysis of the Fab fragment from human immunoglobulin New at 2.0 Å resolution. *J. Biol. Chem.* 253:585–597.
- Sternberg, M. J. E., and J. M. Thornton. 1977. On the conformation of proteins: an analysis of  $\beta$ -pleated sheets. *J. Mol. Biol.* 110:285–296.
- Suezaki, Y., and N. Gö. 1975. Breathing mode of conformational fluctuations in globular proteins. *Int. J. Pept. Protein Res.* 7:333–334.
- Zhou, G. P. 1981. Vibrational energy of ringlike DNA molecules. *Shengwu Huaxue Yu Shengwu Wuli Jinzhan.* 5:19–22.